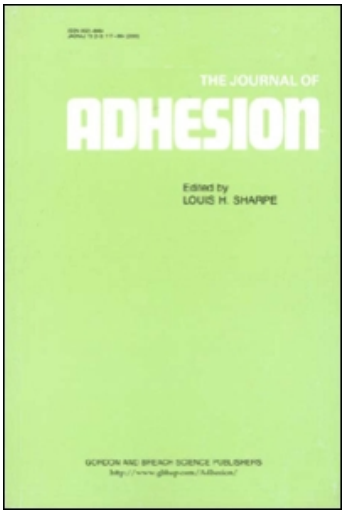

The Journal of Adhesion
Publication details, including instructions for authors and subscription information:
http://www.informaworld.com/smpp/title~content=t713453635

Quantifying the Relationship Between Peel and Rheology for Pressure Sensitive Adhesives

David J. Yarusso[a]
[a] 3M Center, 3M Company, St. Paul, MN, USA

To cite this Article Yarusso, David J.(1999) 'Quantifying the Relationship Between Peel and Rheology for Pressure Sensitive Adhesives', The Journal of Adhesion, 70: 3, 299 — 320
To link to this Article: DOI: 10.1080/00218469908009561
URL: http://dx.doi.org/10.1080/00218469908009561

J. Adhesion, 1999, Vol. 70, pp. 299–320
Reprints available directly from the publisher
Photocopying permitted by license only

Quantifying the Relationship Between Peel and Rheology for Pressure Sensitive Adhesives

DAVID J. YARUSSO*

3M Company, 3M Center, 230-1D-15, St. Paul, MN 55144-1000, USA

(Received 7 August 1998; In final form 4 March 1999)

An attempt is made in this work to model quantitatively the peel force *vs.* rate behavior of a pressure sensitive adhesive (PSA) tape. The approach follows suggestions of previous authors in modeling the deformation of the PSA as uniaxial extension of individual strands. A debonding failure criterion based on stored elastic energy density is used. In this work, experimental measurements of dynamic mechanical master curves are used to provide the mechanical properties of the PSA in the model. The predictions are compared with experimental peel force *vs.* rate master curves on tapes made from those same adhesives. The only adjustable parameter for the fitting is the quantity related to the debonding criterion. In this set of natural-rubber-based PSAs, the general shape of the peel master curve and the changes in peel behavior associated with tackifier loading and rubber molecular weight are well explained by the model. The effect of changes in substrate chemistry are not well explained.

Keywords: Pressure sensitive adhesive; PSA; peel mechanics; viscoelasticity; rheology; modeling; rubber; resin; tackifier

INTRODUCTION

In the pressure sensitive adhesive (PSA) area, much has been written about the connection between the rheological properties of the adhesive and the adhesive performance, especially the peel force, tack, and shear resistance. Dahlquist [1] proposed a minimum level of compliance at the 1-sec time scale as a necessary requirement for

*Tel.: 651-736-1878.

pressure sensitive tack. Chang [2] proposed the "viscoelastic window" concept to define the utility of pressure sensitive adhesives based on values of their dynamic mechanical properties at two time scales. The relationship between dead load shear resistance of a pressure sensitive tape and the shear creep compliance has also been analyzed in detail by Dahlquist [3]. The effects of formulation such as incorporation of tackifiers and oils on the rheological properties and the performance have been examined by a number of authors [4–6]. The rheological properties and peel force *vs.* rate curves for rubber-tackifier blend systems were investigated in detail by Aubrey and Sherriff [7, 8].

A quantitative relationship between rheological properties and peel force has been elusive, however. It is clear that the peeling process involves a coupling of the strength of the interaction across the adhesive/substrate interface and the bulk rheological properties of the adhesive. The fracture energy of PSA peeling is orders of magnitude higher than the thermodynamic work of adhesion for the interface under most circumstances. However, the magnitude of that fracture energy seems to be roughly proportional to the work of adhesion. Some workers have attempted to measure the interfacial energy by using crosslinked rubber, high temperatures, and very slow deformations to try to minimize the viscoelastic contribution [9, 10]. Andrews [11], Gent [12] and others argue that the peel force can be understood as a product of the work of adhesion and a viscoelastic function of rate and temperature which is dependent on the adhesive rheological properties. However, it is not clear how that viscoelastic function should be related to measurable properties.

One approach to the quantitative treatment of this coupled problem was proposed by Hata [13]. He suggested that one could approximate the deformation of the PSA as uniaxial extension of independent adhesive strands and that the adhesive's rheological properties could be approximated by a set of parallel Maxwell elements. He argues that the qualitative features of peel can be predicted if one assumes that the failure criterion for debonding of these extended adhesive strands from the substrate is based on reaching a critical value of the stored elastic energy density in the strand. The peel force is directly related to the total work done on the adhesive strand up to this debond point by a simple energy balance. In the referenced work, he showed detailed results for two elements but suggested the generalization to any

number necessary to describe adequately the relaxation time spectrum of the material. More recently, Mizumachi, Hatano, and Tsukatani [14–16] have applied this method to the problem of predicting the rolling friction coefficient of PSAs as a function of speed and temperature and have provided modifications to account for the bonding process as well as the debonding process. These authors have concentrated on using the two-element model and treating the parameters of the Maxwell element models (the two moduli and time constants) as fit parameters to the rolling friction coefficient data.

In this paper, Hata's approach is applied to the prediction of peel force *vs.* peel rate master curves for PSAs. Rather than using the Maxwell model parameters as fit parameters, however, the author obtains the Maxwell model description of the adhesive properties from linear viscoelastic measurements and then attempts to fit the measured peel force data in the interfacial failure regime using only the single parameter associated with the debonding failure criterion as the fit parameter. The approach is applied to data on a set of natural-rubber-based adhesives peeling from stainless steel and from a moderate release surface (the backside of a commercial packaging tape).

EXPERIMENTAL METHODS

Natural rubber pressure sensitive adhesives were prepared using of two base rubber solutions. One was made by dissolving a controlled viscosity grade of natural rubber, SMR CV60, directly in toluene with no prior mastication of the rubber. The CV60 grade of rubber is made by addition of hydroxyl amine to the natural rubber latex at the time of coagulation to prevent crosslinking on storage [17]. This system has very high molecular weight but appears to be completely soluble. There may still be some microgel content, however, as is common in natural rubber [18]. The second rubber base was prepared by milling a ribbed smoked sheet (RSS) natural rubber for approximately 10 minutes on a laboratory two-roll mill and then dissolving the milled rubber in toluene. The molecular weight of this material was substantially lower as was obvious from the lower solution viscosity at the same solids content. Both solutions were initially prepared at a solids level of about 20% but the CV60 solutions were then diluted to about 13% to obtain a more manageable viscosity.

Pressure sensitive adhesives were prepared by blending these rubber bases with a toluene solution of Piccolyte™ $S-115$ poly(β-pinene) tackifying resin from Hercules, Inc. and a small amount of Irganox™ 1010 antioxidant from Ciba-Geigy (0.5% of total adhesive mass). The four adhesive mixtures examined are shown in Table I:

To prepare the samples for dynamic mechanical properties testing, the adhesive solutions were coated onto a silicone release liner using a notched bar coater at a thickness of approximately 125 μm and dried in a forced air oven at 65°C for 10 minutes. Circles were cut with a die at 25 mm diameter and adhesive layers were laminated together until a total thickness of approximately 1.5 to 2.0 mm was achieved. These samples were then mounted on the 25 mm parallel plate fixture of a Rheometrics™ RDA-II dynamic mechanical rheometer for testing. The test sequence was a set of frequency sweeps at various temperatures. The angular frequency range was 0.1 to 100 rad/sec in logarithmically-spaced steps with 3 increments per decade. The first temperature range was from -40°C to -10°C in 10°C steps using a strain of 1%. The second temperature range was from 0°C to 60°C in 20°C steps using a strain of 3%. Finally, the range from 80°C to 200°C was covered in 30°C increments using a strain of 10%.

Master curves were constructed by the standard reduced variables procedure [19]. The density ratio correction was ignored but the correction for absolute temperature ratio effect on modulus was included. The lowest temperature in each data set was initially used as the reference temperature. After superposition, the shift factors were fitted to the Williams-Landel-Ferry [20] (WLF) equation and then the value of the fitted shift factor at 25°C was used to shift the entire master curve to the 25°C reference temperature.

To prepare the samples for peel force testing, the adhesive solutions were coated at a thickness of approximately 25 μm on a piece of

TABLE I Summary of adhesive systems studied

Sample	*Rubber base*	*Piccolyte S – 115 wt%*	*Rubber MW*
A	Milled RSS	40	low
B	Milled RSS	50	low
C	CV60	40	high
D	CV60	50	high

biaxially-oriented poly(ethylene terephthalate) film (PET) which had been previously coated with a proprietary primer and backside release system. The adhesive was dried in a forced air oven at 65°C for 5 minutes. The adhesive surface was covered with the release coated backside of a creped paper backing used for Scotch Brand™ #233 masking tape.

The peel force *vs.* peel rate data were generated at various speeds and temperatures using a Sintech® universal testing machine equipped with an environmental chamber. The chamber was cooled by direct injection of liquid CO_2 into the chamber and heated electrically with forced internal circulation of the air. The temperature controller used time proportioning of the heater and the CO_2 solenoid to maintain temperature to within 1°C of the set point. The adhesive tapes were applied to a polished stainless steel panel which had been cleaned with one wipe of heptane followed by one wipe with ethanol followed by three more wipes with heptane using Kimwipes™ tissues. The tapes were rolled down using two slow (approximately 30 in/min) (76 cm/min) passes (one forward and one back) of a 2 kg rubber covered roller. A 5 lb (11 kg) load range transducer was used for these measurements. For some of the measurements, the test substrate was the release-coated side of a piece of commercially available box sealing tape, Scotch #355. For those measurements, the box sealing tape was unwound several wraps and applied to the stainless steel panel. The tape was rolled down by the same procedure as described above, taking care not to allow fingers to come in contact with the tape backside. Then the test tape was applied to the backside of the box sealing tape and rolled down. The same equilibration procedures were used as for testing on stainless steel. Because the box sealing tape is adhered to the test panel using its own adhesive, it is possible that deformation occurring in the box sealing tape adhesive may contribute to the performance of the test tape peeling from the release surface. In this case, the glass transition temperature and modulus of the box sealing tape adhesive are both higher than the corresponding values for the test tape, so we believe that the box sealing tape adhesive is effectively rigid under the test conditions and have neglected its possible effects.

For test temperatures below room temperature, the tape was allowed to dwell at 23°C for 5 min before mounting in the chamber. In all cases, the panel was allowed to equilibrate in the chamber at the

desired test temperature for 10 minutes after the chamber reached the set point. The tapes were stripped back in a 180° peel mode with crosshead speeds ranging from 0.05 to 50 in/min (0.13 – 127 cm/min). All the peel speeds were obtained on a single test specimen usually in the following order: 50, 5, 0.5, 0.05, 20, 2, 0.2 in/min. At the slowest testing speeds, we found a reproducible offset of about 20% between the set speed and the actual speed as indicated by the crosshead travel distance and elapsed time. The actual speeds are used in all data presentations. The set of temperatures used included −10, 5, 22, 60 and 100°C. The failure mode was recorded based on visual observation as either interfacial (no obvious tacky adhesive layer left on panel), cohesive (obviously tacky layer left on panel), or mixed. No attempt was made to determine whether small quantities of adhesive residue were present on the panel during apparently "interfacial" failure.

The peel force master curves were constructed using the WLF shift factor function determined from the rheological testing, not from empirical shifting of the peel data. As is the accepted practice, the peel values were corrected for the absolute temperature ratio between the test temperature and the reference temperature prior to horizontal shifting [21].

MODEL DEVELOPMENT

If one accepts the concept of treating the adhesive deformation as approximated by uniaxial extension of strands, one can qualitatively evaluate various possible strand detachment criteria for agreement with existing data. To do so, one needs only a crude description of the rheological behavior of the adhesive and a simple model with two parallel Maxwell elements will do. The high-modulus element is chosen to have a modulus characteristic of the glassy regime and the low-modulus element that of the rubbery plateau. The relaxation times of the elements are chosen to correspond roughly to the transition frequencies for the glass-to-rubber transition and for the rubber-to-liquid flow transition.

One possible failure criterion would be to assume that the adhesive deforms until a certain critical stress is reached. Such a criterion can predict the transition from cohesive to interfacial failure [22] but in the interfacial regime it predicts a peel force which decreases continuously with increasing rate. Such behavior is never observed in PSAs.

Another possible criterion for strand debonding would be a critical strain level. However, the result of such a criterion is a peel force which increases with rate without bound. This is also physically unrealistic.

At first, this author thought it might be more reasonable to base the debonding criterion on a critical value for the total stored elastic energy in the system rather than the energy density as suggested by Hata [13]. It was hoped that through such an approach one could directly connect the critical value of this stored energy to the work of adhesion.

However, the result of such a postulate is a predicted peel force which is independent of adhesive thickness. There exist considerable data to suggest that over most of the range of useful thickness of PSAs, the peel force is roughly proportional to thickness [23].

Using Hata's critical stored elastic energy density failure criterion coupled with the simple two parallel Maxwell element model of the adhesive rheology gives qualitative agreement with the observed experimental data. The peel force is proportional to adhesive thickness. At low rates one predicts cohesive failure with a peel force which rises with peeling speed. At a certain speed a transition to interfacial failure is predicted which may or may not be accompanied by a drop in the peel adhesion, depending on the magnitudes of the parameters. The peel force increases with speed in the interfacial failure zone and finally goes through a maximum. The region where the predicted peel force drops with increasing speed would be expected to be unstable and to give rise to the stick-slip peel which is observed.

The primary fault with the model as described is that the peel force rises too suddenly in the region prior to the transition to unstable peel. We believed that this was primarily due to the unrealistic approximation of the adhesive rheology by a two-element model. For that reason we chose to follow Hata's suggestion and employ a generalized Maxwell model description of the adhesive rheology, obtaining the parameters of the model from the measured dynamic mechanical properties. Such a model is shown in Figure 1.

The response of such a model to a uniaxial extension at constant end separation speed (such as in a typical stress-strain test) is given by:

$$\sigma(t) = R \sum_{i=1}^{n} E_i \theta_i (1 - e^{-t/\theta_i})$$

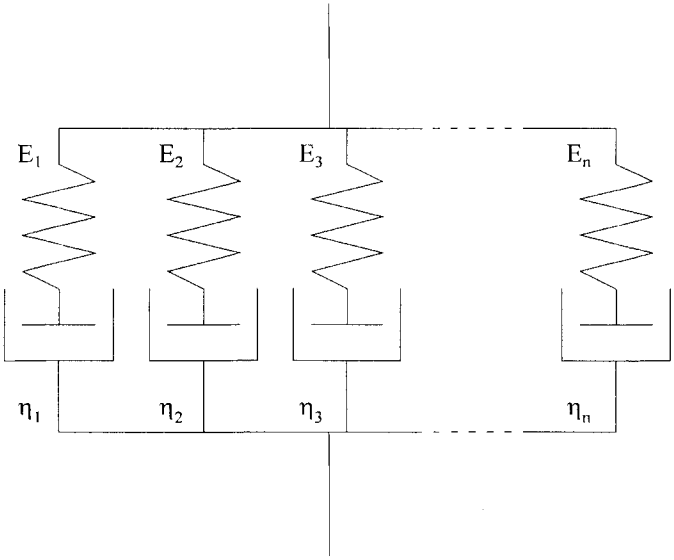

FIGURE 1 Schematic representation of generalized Maxwell model.

where:

σ ten sile stress
t time
R separation speed (crosshead speed)
E_i modulus of Maxwell element i
θ_i time constant of element, i η_i/E_i
n number of elements in model

The stored elastic energy density during uniaxial constant rate extension can be calculated as the sum of the energy stored in the springs of all the elements:

$$U(t) = \frac{R^2}{2} \sum_{i=1}^{n} E_i \theta_i^2 (1 - e^{-t/\theta_i})^2$$

where:

U stored elastic energy density (energy per unit volume)

The total work done on an adhesive strand per unit volume of adhesive is given by the integral of the stress-strain curve. For the

constant separation rate case,

$$\varepsilon = Rt \quad \text{and}$$

$$W = R^2 \sum_{i=1}^{n} \eta_i \left[t - \theta_i \left(1 - e^{-t/\theta_i} \right) \right]$$

where:

ε elongation, $\Delta l/l_0$
W total work done on strand (energy per unit volume)
η_i viscosity of Maxwell element i

Following the postulate of Hata, we assume that there is a critical value of the stored elastic density, U_c, at which the strand detaches from the surface. For this generalized Maxwell model, there is a minimum deformation rate below which one can never reach U_c. When the deformation is slow enough, the springs do not extend very much. Essentially all of the strain is in the dashpot elements. We interpret this rate as the rate below which cohesive splitting of the strand will occur. If we want to calculate a peel force in the cohesive failure regime, we must postulate a new failure criterion for this region. In the present work, we have assumed that the strand will break if it reaches a critical value of the elongation of the strand, *i.e.*, the break elongation, ε_b. Other possible failure criteria for the cohesive failure regime were not evaluated.

To calculate peel force at a given peeling speed, we assume that the deformation of the adhesive in the peel nip can be approximated as uniaxial extension of individual adhesive strands with a constant rate of end separation which is equal to the rate of peel front propagation. We further assume that all the adhesive on the tape takes part in the deformation to the same extent. Thus, to calculate the peel force at a certain speed we determine the peel front propagation rate which, for 180° peel, is one-half the peeling speed. We then begin calculating the stored elastic energy density and the total work done on the strand according to the equations provided above while incrementing the time. When the stored elastic energy density reaches the critical value, U_c, we assume that the strand detaches. If the break elongation value is reached first, we assume that the adhesive has failed by cohesive splitting. In either case, the total work done up to that point per unit

volume of adhesive, W, is directly proportional to the peel force by an overall energy balance. For 180° peel:

$$Fd = Whb\frac{d}{2} \quad \text{or}$$

$$\frac{F}{b} = \frac{Wh}{2}$$

where:

F Peel force
d peel distance
h adhesive thickness
b tape width

The calculation is repeated for as many peel rates as one wishes to predict.

RESULTS AND DISCUSSION

The dynamic mechanical master curves for the four adhesives used in this study are shown in Figure 2. The lower molecular weight of samples A and B is evident from the depression of the G' curve at low frequency compared with the higher molecular weight Samples C and D. The classical effects of adding tackifying resin are seen in comparing curve B with A and curve D with C. The plateau modulus is reduced and the transition to glassy behavior occurs at a lower frequency in the presence of higher amounts of the tackifier. The WLF constants determined by fitting the shift factor *vs.* temperature dependence are shown in Table II.

The following procedure was used to extract the generalized Maxwell model parameters from these data. First, the data were smoothed by fitting both the G' and the G'' master curves to 8th order polynomials. Then, the methods of Ninomiya and Ferry [24] were used to obtain approximate relaxation spectra, $H(\tau)$. These methods involve numerical differentiation of the G' and G'' functions. There are two separate procedures, one obtaining the spectrum form G' and one from G''. In principle these two should agree if the data are self-

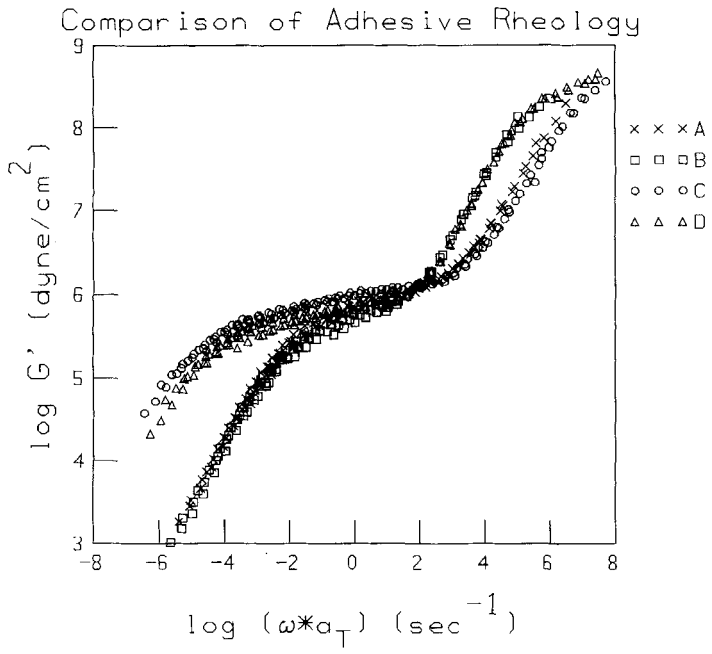

FIGURE 2 Comparison of G' master curves for adhesive samples A, B, C and D.

TABLE II WLF Parameters of adhesives reference temperature is 25°C

Sample	*C1*	*C2*
A	8.07	147.1
B	8.03	128.1
C	10.93	176.4
D	9.90	153.9

consistent. The spectra calculated by both methods are shown in Figure 3 through Figure 6 for the four adhesives. There is close agreement with the exception of sample D, for which there is a region at intermediate time constants where the spectra calculated by the two methods diverge. For the purpose of the modeling, we chose to average the results of these two methods.

The model described above was used to calculate peel force *vs.* peel rate curves using the value of U_c and ε_b as adjustable parameters of fit.

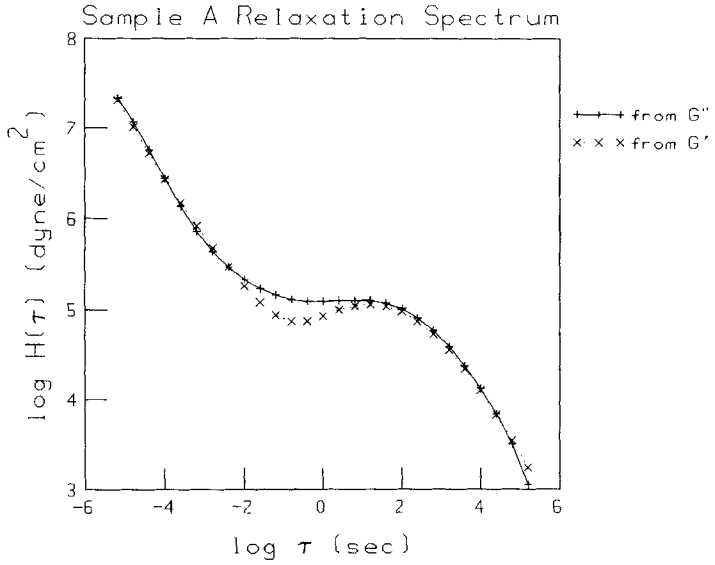

FIGURE 3 Relaxation spectrum for Sample A.

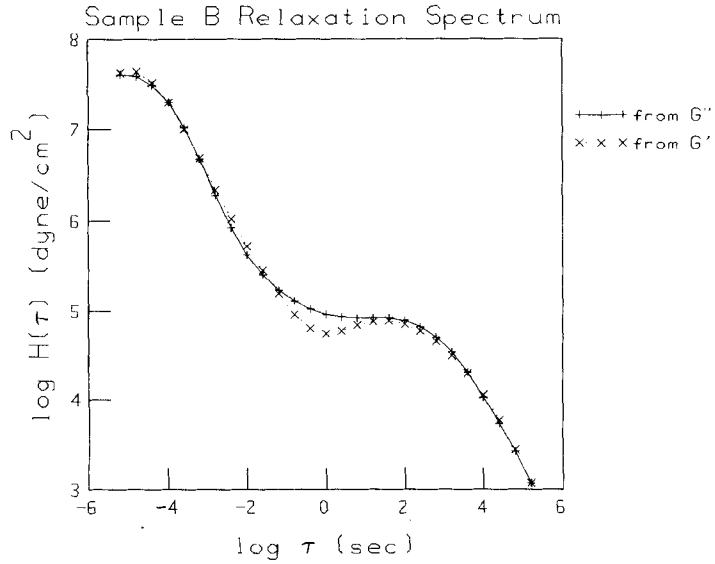

FIGURE 4 Relaxation spectrum for Sample B.

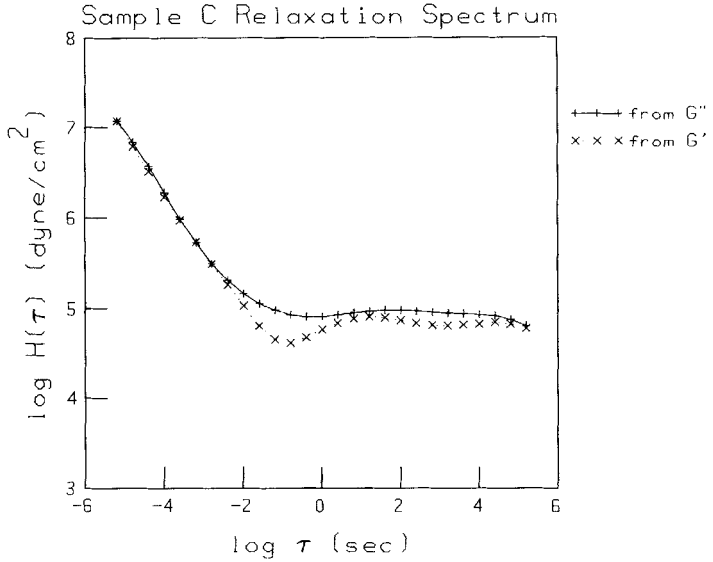

FIGURE 5 Relaxation spectrum for Sample C.

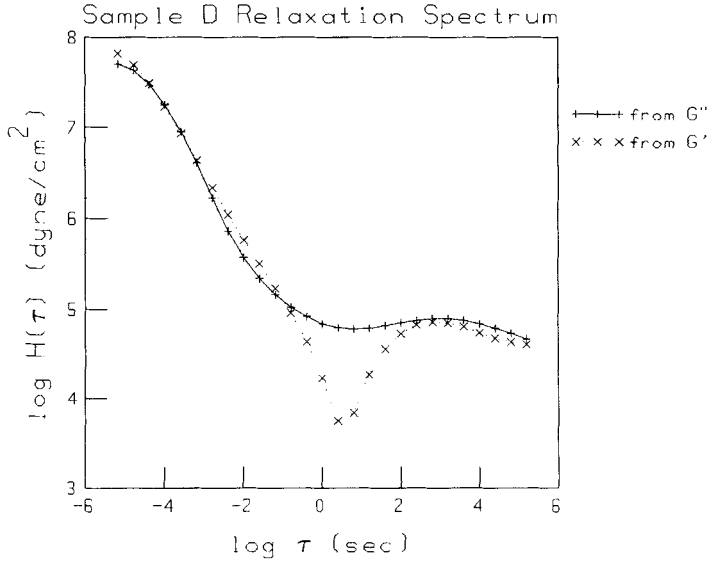

FIGURE 6 Relaxation spectrum for Sample D.

The value of U_c affects the magnitude of the peel curve in the interfacial failure zone and has a slight effect on the peak position, with higher values leading to higher peel forces and slightly higher "shocky" peel transition rates. The value of ε_b affects the magnitude of the peel force in the cohesive failure region and the position of the transition from cohesive to interfacial peel, with higher values leading to higher peel force and lower rate of transition from cohesive to interfacial failure. Since the value of U_c according to the model ought to be dependent only on the strength of the interfacial bond, and since all these adhesives should be identical in the chemical nature of the interface on a given substrate, we attempted to find a single value which would adequately fit the data for all the adhesives on a given substrate. We also found that reasonably good agreement could be obtained for all the adhesives using a single value of ε_b. The data and model fits are shown in Figure 7 through Figure 10. The values of U_c and ε_b used are summarized in Table III.

Note that for samples A and B, which are prepared from the lower molecular weight rubber, the model seems to fit the data reasonably well. When the value of U_c is adjusted to agree with the magnitude of

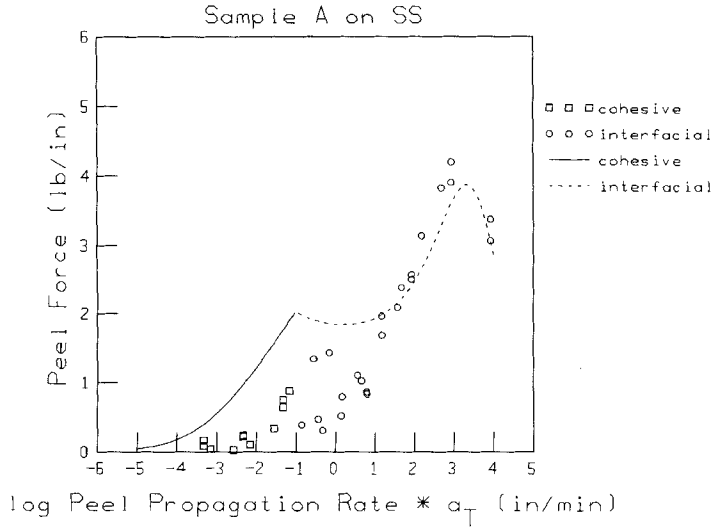

FIGURE 7 Model fit to peel master curve data for Sample A peeling from stainless steel.

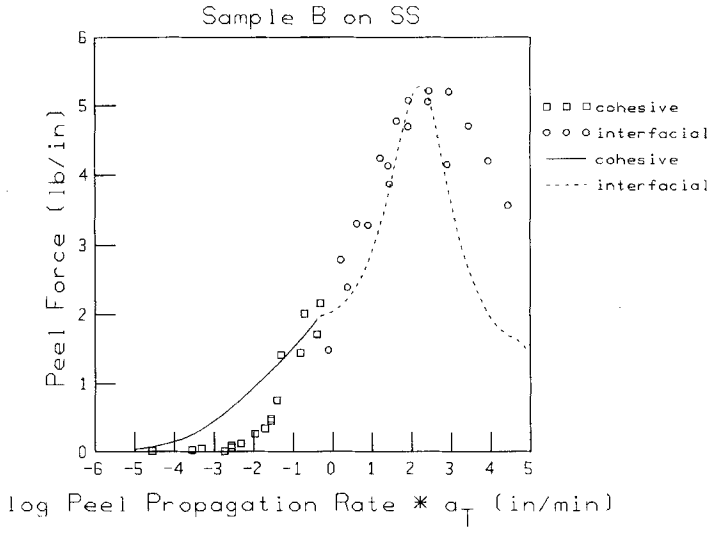

FIGURE 8 Model fit to peel master curve data for Sample B peeling from stainless steel.

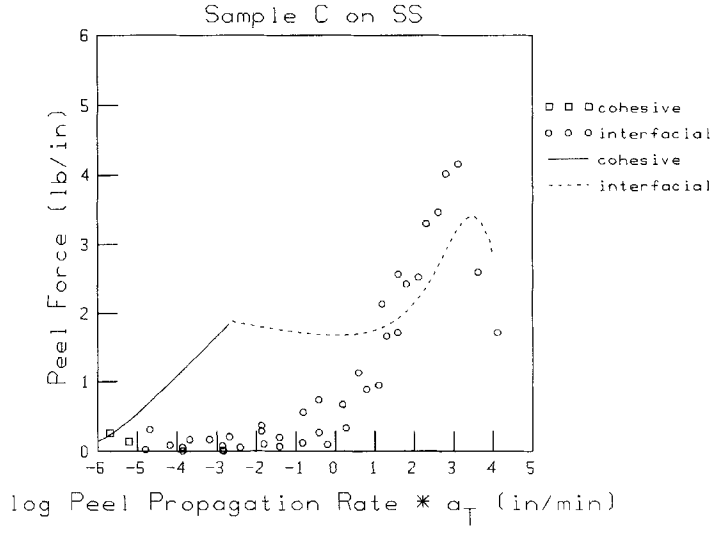

FIGURE 9 Model fit to peel master curve data for Sample C peeling from stainless steel.

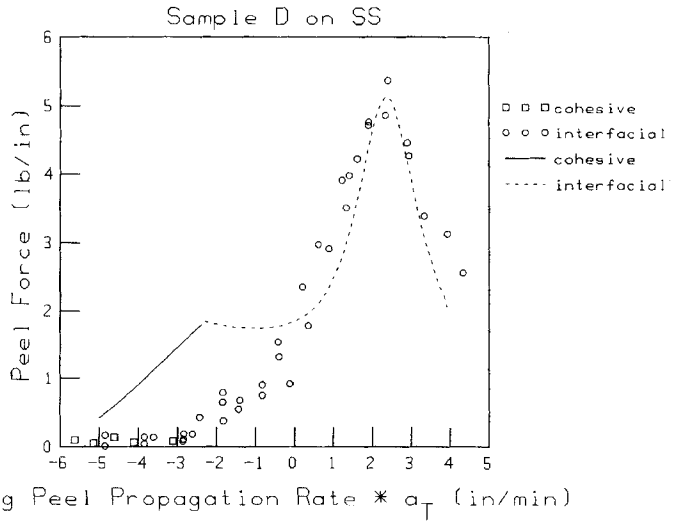

FIGURE 10 Model fit to peel master curve data for Sample D peeling from stainless steel.

TABLE III Summary of parameters used for peel modeling

Adhesive	*Substrate*	U_c J/cm^3	ε_b
A	stainless steel	7.0	10
B	stainless steel	7.0	10
C	stainless steel	7.0	10
D	stainless steel	7.0	10
A	#355 tape backside	2.0	10
B	#355 tape backside	2.0	10
C	#355 tape backside	2.0	10
D	#355 tape backside	2.0	10

the peel force curve, the peak position is predicted quite nicely. The value of ε_b was adjusted primarily to get the right position of the transition from cohesive to interfacial failure. Under those conditions, the model does seem to overpredict the magnitude of the peel force in the cohesive failure zone. In sample A, the model also overpredicts the peel force in the low speed region of the interfacial failure zone.

For the higher molecular weight materials, C and D, the model does not do quite as well. The transition to shocky peel from stainless steel

is still matched fairly closely but the experimental data fall to very low peel forces at low peeling speed while the model predicts substantial peel adhesion in this region. Furthermore, for Sample C, the model predicts a transition to cohesive failure at a considerably higher rate than where it is in fact observed. This aspect of the fit is considerably better for Sample D.

When we look at the data and model predictions for peeling from the release surface of the #355 box sealing tape in Figure 11 through Figure 14, we see that the transition to shocky peel occurs at a much lower rate in the data than predicted by the model. Such a large reduction in shocky peel transition rate on a low energy surface is rather typical of pressure sensitive tape behavior and can be seen in the data of Kaelble [21] for peeling of an acrylic adhesive from many surfaces, including polytetrafluoroethylene (PTFE). In that work, the peel master curve on PTFE exhibits a shocky peel transition rate about two orders of magnitude lower than that for peeling from glass. Although the modeling approach used here does predict a small shift downward in the rate of transition to shocky peel upon reduction of U_c, it is not nearly as large as the observed shift. By comparison,

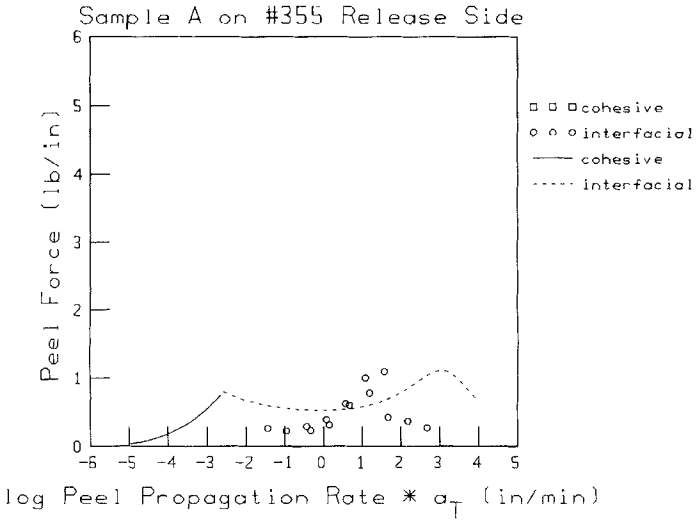

FIGURE 11 Model fit to peel master curve data for Sample A peeling from backside of #355 box sealing tape.

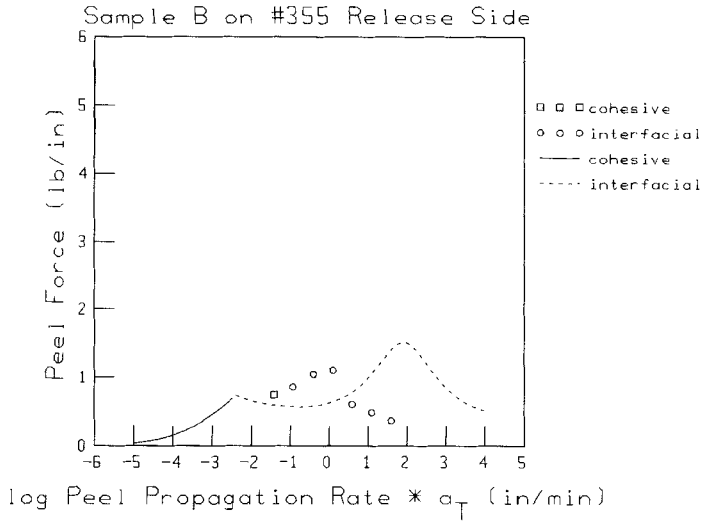

FIGURE 12 Model fit to peel master curve data for Sample B peeling from backside of #355 box sealing tape.

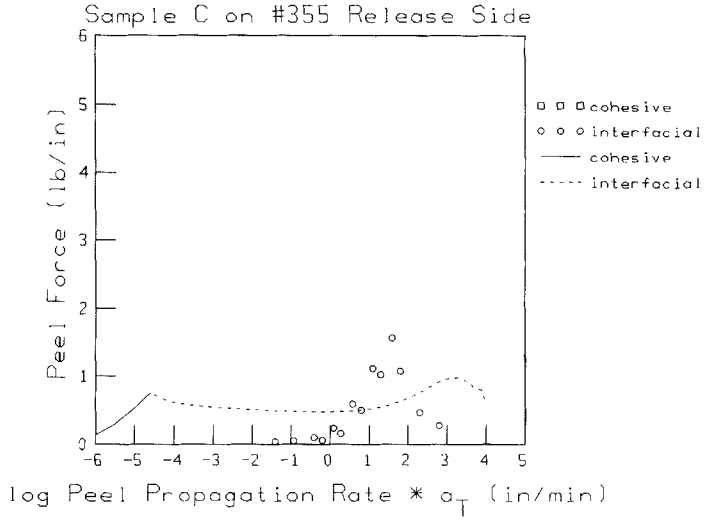

FIGURE 13 Model fit to peel master curve data for Sample C peeling from backside of #355 box sealing tape.

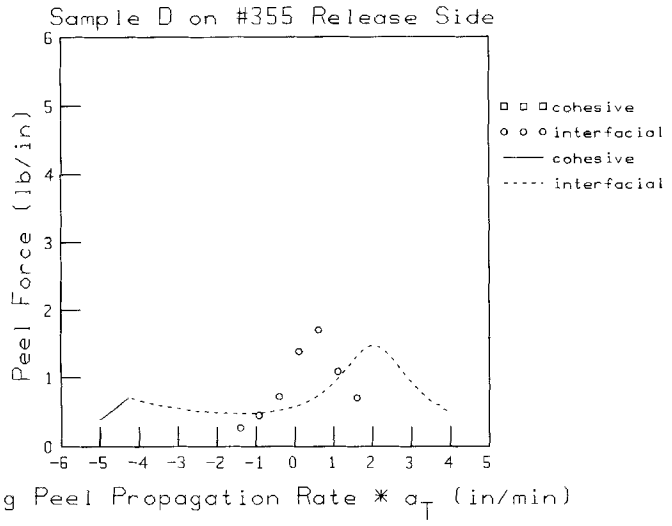

FIGURE 14 Model fit to peel master curve data for Sample D peeling from backside of #355 box sealing tape.

however, the approach of Andrews [11] would predict no shift at all. A possible reason for the failure of the model in this area is that the relative importance of filament elongation in the peel process depends on the strength of the interface. It was observed in this work that when peeling from the stainless steel, adhesive strands were visible over much of the range of test conditions whereas, from the release surface, such stranding was suppressed.

With regard to the peeling from stainless steel, the key failing of the model seems to be in the low peel rate regime, especially for the high molecular weight adhesives. One possible source of difficulty here may be that the rheological measurements we made still fail to provide information on the longest time constants in the adhesive. One can see from the relaxation time spectra on the high molecular weight Samples (C and D) that we have not gone far enough to see the contributions of long-time components drop to negligible values. The experimental limitation here is the maximum temperature which the sample can tolerate without suffering degradation.

One can postulate many other reasons why this model does not work perfectly. The break elongation may be rate dependent, the

critical elastic energy density value may be rate dependent, the model does not take into account large strain properties of the adhesive, the adhesive does not actually deform as independent strands in uniaxial tension, not all of the adhesive may participate equally in deformation and the nature of the adhesive deformation may be rate dependent, to name a few. This author finds it remarkable that the model works as well as it does, given the complexity of the actual situation and the simplicity of the model.

Ultimately, one would like to be able to connect the value of the critical stored elastic energy density, U_c, (energy per unit volume of adhesive) to the strength of the interfacial interaction or the thermodynamic work of adhesion, W_a (energy per unit area of bond). If there is to be a relationship between these quantities, there must be a characteristic length scale to connect them. If we assume that the work of adhesion for the adhesive/stainless steel interface is about 50 erg/cm^2, and we assume that

$$U_c \cdot l = W_a$$

then the characteristic length scale, l, needs to be about 7 nm to explain our U_c value of 7 J/cm^2. The author has no ready explanation for the meaning of this length scale but it is interesting that it is of the right order of magnitude to correspond to an entanglement spacing. In fact, using the value of the average molecular weight per entanglement from Ferry, $M_e = 6100$ g/mol and taking account of the dilution effect of the tackifier in our formulation with a rubber fraction of 60%, following Graessley's argument [25] that the entanglement spacing varies with the square of the rubber fraction, one can calculate that the length of the edge of a cube containing on average one entanglement is 3 nm. This is certainly close to the value for the length scale obtained above. Perhaps only that portion of a chain between the interface and the nearest entanglement can relax quickly enough to play a role in the local debonding process. Alternatively, this length scale might be interpreted as a interfacial flaw dimension by analogy to linear elastic fracture mechanics arguments. Future work examining other adhesive systems of different entanglement spacing and peel experiments with varied roughness might help to elucidate this issue.

CONCLUSIONS

The proposed model provides semi-quantitative agreement with the data for peel of natural rubber-resin adhesives from stainless steel. The connection between linear viscoelastic properties of the adhesive and the dependence of peel force on rate is made rather simply using this model, even though the shape of the peel force *vs.* rate curve bears little resemblance to any one of the simple viscoelastic functions.

A key failing of the model is its inability to explain the fact that when peeling from low energy releasing surfaces the transition to shocky peel occurs at a much lower speed.

Further work in which the adhesive debonding zone geometry is analyzed directly during peeling could be useful for identifying the failings of the model and testing the predictions of strand elongation along with whose of peel force.

References

[1] Dahlquist, C. A., *Proc. Nottingham Conf. on Adhesion* (MacLaren and Sons, Ltd. London, 1966), Part III, Ch. 5, p. 134.
[2] Chang, E. P., *J. Adhesion* **34**, 189 (1991).
[3] Dahlquist, C. A., Chapter 6 in *Handbook of Pressure Sensitive Adhesive Technology* Satas, D., Ed. (Van Nostrand Reinhold, New York, 1989).
[4] Class, J. B. and Chu, S. G., *J. Appl. Poly. Sci.* **30**, 805 (1985).
[5] Class, J. B. and Chu, S. G., *J. Appl. Poly. Sci.* **30**, 815 (1985).
[6] Class, J. B. and Chu, S. G., *J. Appl. Poly. Sci.* **30**, 825 (1985).
[7] Aubrey, D. W. and Sherriff, M., *J. Polym. Sci., Polym. Chem. Ed.* **16**, 2631 (1978).
[8] Aubrey, D. W. and Sherriff, M., *J. Polym. Sci., Polym. Chem. Ed.* **18**, 2597 (1980).
[9] Gent, A. N., *Rubber Chem. Technol.* **55**, 525 (1982).
[10] Johnson, K. L., Kendall, K. and Roberts, A. D., *Proc. Roy. Soc. Lond.* **A324**, 301 (1971).
[11] Andrews, E. H. and Kinloch, A. J., *Proc. Roy. Soc. Lond.* **A332**, 385 (1973).
[12] Gent, A. N. and Lai, S.-M., *J. Poly. Sci.: Part B: Polymer Physics* **32**, 1543–1555 (1994).
[13] Hata, T., *J. Adhesion*, **4**, 161 (1972).
[14] Mizumachi, H., *J. Appl. Poly. Sci.* **30**, 2675 (1985).
[15] Mizumachi, H. and Hatano, Y., *J. Appl. Poly. Sci.* **37**, 3097 (1989).
[16] Tsukatani, T., Hatano, Y. and Mizumachi, H., *J. Adhesion* **31**, 59 (1989).
[17] St.Cyr, D. R., Chapter in *Encyclopedia of Polymer Science* 2nd edn. Vol. 14 (Wiley and Sons, NY, 1988), p. 687.
[18] Subramaniam, A., *Rubb. Res. Inst. Malaysia Technol. Bull.* No. 4 (1980).
[19] Ferry, J. D., *Viscoelastic Properties of Polymers* 3rd edn. (Wiley and Sons, New York, 1980), Chap. 11.
[20] Williams, M. L., Landel, R. F. and Ferry, J. D., *J. Am. Chem. Soc.* **77**, 3701 (1955).

[21] Kaelble, D. H., *J. Adhesion* **1**, 102 (1969).
[22] Gent, A. N. and Petrich, R. P., *Proc. Roy. Soc. Lond.* **A310**, 433 (1969).
[23] Kaelble, D. H., *J. Adhesion* **37**, 205 (1992).
[24] Ninomiya, K. and Ferry, J. D., *J. Colloid Sci.* **14**, 36 (1959).
[25] Graessley, W. W., *Adv. Polym. Sci.* **16**, 1 (1974).